

## Network Based Signal Recovery in Wireless Networks.

<sup>1</sup>Mr. Mustak Pasha, <sup>2</sup>Prof. Asma Parveen  
<sup>1</sup>(Computer Science and Engineering, KBNCE/VTU Belgaum, India)

**ABSTRACT :** One of the severe problems in wireless interaction is the interference. Interference is caused due to collision. In wireless network, the signal sent by a node will reach all its neighboring nodes. The signal will collide, if a neighbor apart from the target node is receiving data from more than one node at the same moment then the required signal will get cracked, which result in communication crash. In conventional wireless networks, this crash of signals may cause communication failure if no division procedure is accepted. This will corrupt the system performance, which include packet loss rate and energy effectiveness. In traditional transmission when a terminal is receiving messages, its neighbors cannot transmit until receiving is finished, such a mechanism is not efficient and a lot of bandwidth is wasted. The inefficiency of traditional wireless transmission is mainly due to regulating the signal collision. In dispersed network such as ad hoc and some sensor networks, the organize hub will not present in the network. This will increase the clash and interference. In wireless networks, when signal crash, electromagnetic waves will overlap on each other. This strategy is much more practical and easier to realize. Neither strict synchronization nor power control is needed among the different terminals

**KEYWORDS** -Block fading, network coding, scheduling, time variant and wireless network.

### I. INTRODUCTION

The BROADCAST nature of wireless medium is one of the principal features of wireless networks. Although this feature may somewhat facilitate the broadcast communication, it usually causes interference and collision in other scenarios. In a wireless network, signals sent by a terminal can reach all its neighbors, whereas a terminal may simultaneously receive the signals from all its nearby nodes. In traditional wireless networks, this collision of signals may cause transmission failure if no division technique is adopted. This will degrade the system performance, such as the packet loss rate and energy efficiency. Moreover, in distributed networks such as ad hoc and some sensor networks, the absence of control center will increase the opportunity of collision and interference, which further reduces the transmission rate and brings about the inevitable hidden- and exposed-node problems. Previous solutions to this problem mainly focused on how to avoid signal collision through some well-developed protocols on the medium access control or network layer.

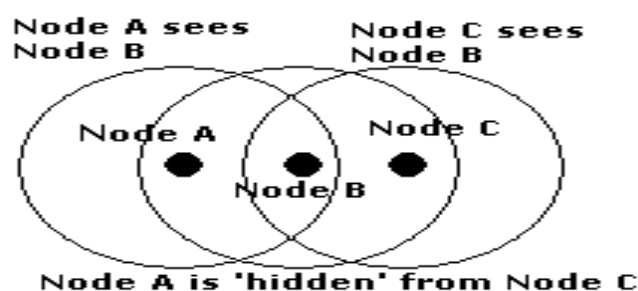


Fig. 1. The hidden nodes problem

For example, shown in Fig. 1, the hidden node problem occurs in a point to multi-point network and is defined as being one in which three (or more nodes) are present. Node A, Node B and Node C. It is possible that in this case Node B can hear Node A (and vice versa) and Node B can hear Node C (and vice versa) BUT Node C cannot hear Node A. In a CSMA/CA environment Nodes A and C would both properly transmit (they cannot hear each other on the 'listen' phase so could both simultaneously and properly transmit a packet) but Node B would get corrupted data. Nodes A and C are said to be 'hidden' from each other.

The hidden nodes problem in wireless multi-hop sensor networks was mainly addressed with two techniques: RTS/CTS and Carrier Sense Tuning .RTS/CTS was basically designed to reduce the number of collisions due to hidden nodes by reserving the channel around both the sender and the receiver to protect frame transmission from being corrupted by hidden nodes. However, this method presents several problems when used in wireless multi-hop sensor networks:

- The energy consumption related to a RTS/CTS exchange is significant, data frames are usually small, the collision probability is the same for data frames as for RTS/CTS, so it does not make any difference if the technique is used or not
- It does not avoid collisions in multi-hop networks
- It may lower the network capacity due to the exposed node problem,
- It cannot be used for broadcast frames.

Several MAC protocols have proposed to use Carrier Sense Tuning to cope with the hidden node problem .The key idea comes from the observation that hidden nodes cause Collisions, because their radio carrier sense range is not large enough to sense ongoing transmissions they may collide with. Hence, a node should tune its radio carrier sense range to make sure that when it transmits, there is no another transmission. Although this method allows a node to detect ongoing transmissions, it is not suitable for all situations. For example, it assumes a homogeneous radio channel for all nodes, which is not always possible because of obstacles, different antenna height, etc. Even if the channel is homogeneous, it is not possible to increase the carrier sense range of radio transceivers indefinitely due to physical limitations.

### 1.1 Use of RTS and CTS

Hidden Nodes are solved by the use of a RTS (request to send)/CTS (clear to send) protocol prior to packet transmission. In our three node network above Node A sends a small RTS packet which is heard by Node B which send a small CTS packet which is heard by both Nodes A and Node C. Node C will not transmit in this case.

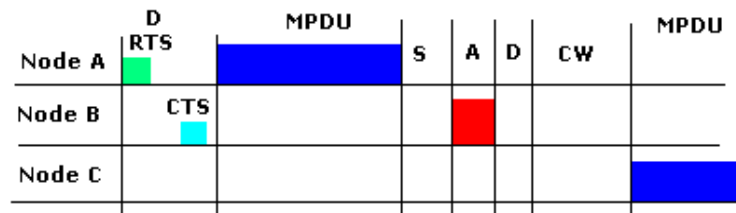


Fig. 2. Use of RTS/CTS protocol prior to packet Transmission

### 1.2 Node Identification

Each node in a 802.11 network is identified by its MAC address (exactly the same as Ethernet a 6 byte - 48 bit value). Receiving nodes recognize their MAC address. A node wishing to send data initiates the process by sending a Request to Send frame (RTS). The destination node replies with a Clear To Send frame (CTS). Any other node receiving the RTS or CTS frame should refrain from sending data for a given time (solving the hidden node problem). The amount of time the node should wait before trying to get access to the medium is included in both the RTS and the CTS frame. This protocol was designed under the assumption that all nodes have the same transmission ranges. RTS/CTS are an additional method to implement virtual carrier sensing in Carrier sense multiple access with collision avoidance (CSMA/CA). By default, 802.11 rely on physical carrier sensing only which is known to suffer from the hidden node problem. RTS/CTS packet size threshold is 0–2347 octets. Typically, sending RTS/CTS frames does not occur unless the packet size exceeds this threshold. If the packet size that the node wants to transmit is larger than the threshold, the RTS/CTS handshake gets triggered. Otherwise, the data frame gets sent immediately. IEEE 802.11 RTS/CTS mechanism could help solve exposed node problem as well, only if the nodes are synchronized and packet sizes and data rates are the same for both the transmitting nodes. When a node hears an RTS from a neighbouring node, but not the corresponding CTS, that node can deduce that it is an exposed node and is permitted to transmit to other neighbouring nodes. If the

nodes are not synchronized (or if the packet sizes are different or the data rates are different) the problem may occur that the sender will not hear the CTS or the ACK during the transmission of data of the second sender.

In this paper, we shall put forward some efficient signal recovery algorithms without the request of synchronization and power control among multiple data streams. Thus, the strategy is much more practical and easier to realize. With our proposed algorithms, since certain types of signal collision are allowed, the throughput and efficiency of wireless networks can greatly be increased. In different types of wireless channels, the waveforms of the received signals are different, thus requiring different algorithms to recover the useful signals. In this paper, we shall put forward several algorithms for three types of wireless channels.

For additive white Gaussian noise (AWGN) and block-fading channels, where the attenuation is constant during the transmission of one frame, the recovering algorithms for BPSK and  $\pi/4$ -QPSK modulated signals will be developed, respectively, without loss of generality. For the time-variant channel, we must know the amplitude of the interference signal at each sampling time because the attenuation varies during the transmission of one frame. Two algorithms on signal recovery will be proposed for large and small coherent times, respectively. Simulation results will show that the bit error rate (BER) of the recovered signal using our developed schemes is almost the same as the transmission without interference, which proves the effectiveness of our strategy based on network coding. The rest of this paper is organized as follows: The network model and the scheduling strategy based on physical-layer network coding are discussed in Section II. In Section III, we will present the signal-recovery algorithms for AWGN and block-fading channels. In Section IV, two algorithms of signal recovery for time-variant channels will be put forward. The performance of the proposed strategy and some other practical issues are discussed in Section V. Section VI illustrates the simulation results, which demonstrate the effectiveness of our approach. Finally, we conclude this paper in Section VII.

## II. NETWORK MODEL AND THE SCHEDULING STRATEGY

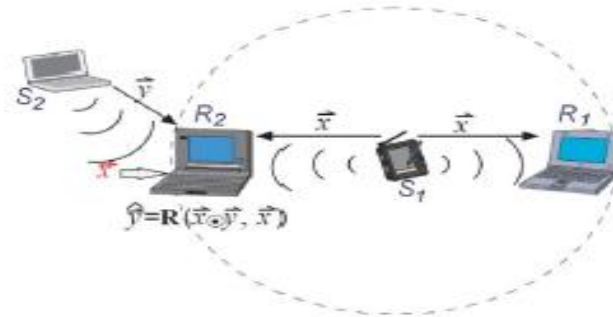


Fig. 3. Model of wireless networks with signal collision.

Our model of wireless networks is shown in Fig. 3, where the source terminals  $S_1$  and  $S_2$  intend to transmit two frames of messages  $\vec{x} = \{x_1, \dots, x_L\}$  and  $\vec{y} = \{y_1, \dots, y_L\}$  to the receivers  $R_1$  and  $R_2$ , respectively.  $L$  is called the “frame length” here. The link between each pair of adjacent terminals is assumed to be half-duplex, which means that each terminal can both transmit and receive messages from its neighbors, but cannot simultaneously do them. Since  $R_1$  and  $R_2$  are both inside the transmission region of  $S_1$ ,  $\vec{x}$  can be received by the two receivers at the same time. If  $S_1$  and  $S_2$  simultaneously transmit, the signal of  $\vec{y}$  will collide with that of  $\vec{x}$  at  $R_2$ , which may result in the transmission failure in traditional systems. However, if  $R_2$  knows the content of  $\vec{x}$ , it can eliminate the interference of  $\vec{x}$  and recover  $\vec{y}$  from the mixed signal. Each multi hop transmission session in wireless networks can well be described by this linear network model. In fact, the model shown in Fig. 3 is a special case. There may be multiple interference signals at  $R_2$ . It will be shown that, as long as the receiver knows the information on all the interference signals, it can recover its desired signal through our algorithms with a very large probability.

For convenience, we only consider the scenario with just one interference signal when we develop the algorithms in the following sections. However, all these algorithms can easily be generalized to the multi-interference case. As mentioned in the previous section, the scheme on signal recovery depends on the channel property. In AWGN and block-fading channels, the attenuation is taken to be constant during the transmission of one frame. Thus, one only needs to estimate the delay and amplitude of the frame of interference signal, and then the interference signal can be “subtracted” from the mixed signal to recover the useful signal. The single-side power spectral density of the additive white noise is assumed to be  $N_0/2$ . For the block-fading channel, the attenuation is assumed to be a Raleigh variable with a mean square value of 1, and different frames are assumed to suffer different and independent attenuations. However, in a general fading channel, if the attenuation varies during the transmission of one frame, we have to estimate the sampling value of each symbol in the frame of the interference signal. To develop an effective signal-recovery algorithm for time-variant channels, an appropriate channel model that can characterize different coherent times is needed. ARMA  $(p, q)$  process is a simple stochastic process model with the aforementioned property. It has been shown that for each random process, one can find an autoregressive moving average (ARMA) process such that its mean square error from the given process is as small as possible if  $p$  and  $q$  are large enough. The generating equation of an ARMA  $(p, q)$  process is

$$A_n + u_1 A_{n-1} + \dots + u_p A_{n-p} = \varepsilon_n + v_1 \varepsilon_{n-1} + \dots + v_q \varepsilon_{n-q} \quad (1)$$

where  $A_i$  is the attenuation at the sampling time  $t_i$ , and  $\varepsilon_i$  is a pure Gaussian random process with mean  $\mu_\varepsilon$  and variance  $\sigma_\varepsilon^2$ . Without loss of generality, we assume that  $\mu_\varepsilon = 0$ . Thus,  $A_i$  is also a Gaussian random variable. Given  $A_{n-1}, \dots, A_{n-p}$  and  $\varepsilon_{n-1}, \dots, \varepsilon_{n-q}$ , the conditional normal distribution function of  $A_n$  is

$$\begin{aligned} p(A_n = z | A_{n-1}, \dots, A_{n-p}, \varepsilon_{n-1}, \dots, \varepsilon_{n-q}) \\ &= \frac{1}{\sqrt{2\pi\sigma_\varepsilon}} \exp \left\{ -\frac{1}{2\sigma_\varepsilon^2} \left( z + \sum_{i=1}^p u_i A_{n-i} - \sum_{j=1}^q v_j \varepsilon_{n-j} \right)^2 \right\} \\ &= \frac{1}{\sqrt{2\pi\sigma_\varepsilon}} \exp \left\{ \frac{1}{2\sigma_\varepsilon^2} (z - \bar{A}_n)^2 \right\} \end{aligned} \quad (2)$$

where  $\bar{A}_n = -\sum_{i=1}^p u_i A_{n-i} + \sum_{j=1}^q v_j \varepsilon_{n-j}$  is the conditional expectation value of  $A_n$ . Since a Raleigh random variable is the sum of the squares of two Gaussian variables with mean 0 and the same variances, both the in-phase and quadrature attenuations of a Raleigh fading channel can be modeled by the ARMA processes. The coefficients  $\{u_i\}$  and  $\{v_j\}$  in (1) can be figured out through the channel estimation, and the values of  $p$  and  $q$  are chosen according to the tradeoff between the accuracy and complexity. If  $q = 0$  in (1), the ARMA process is reduced to an autoregressive (AR) process

$$A_n + u_2 A_{n-1} + \dots + u_p A_{n-p} = \varepsilon_n. \quad (3)$$

The AR process is Markovian, which means that each  $A_n$  is only related to the former  $p$  attenuation values. Since the AR process is easier in form, we will only present the signal recovery algorithms for the channel modeled by the AR process in the latter part of this paper. For the general ARMA process, the algorithms and corresponding deductions are similar. Next, we will briefly discuss the scheduling strategy based on the signal-recovery algorithms. First, each terminal stores the frames it has recently received. Then, we add the identifier of the frame to be sent in the next time slot to the RTS message. Each frame has a unique identifier, which can be defined by the source address and the index of the frame. Thus, the terminal that receives the RTS messages from its neighbors can decide whether they can simultaneously transmit according to the identifier. If among all the frames to be sent there is only one unstored frame, the terminal will broadcast a CTS message; otherwise, the terminal will reply a non-CTS message with the identifiers of the frames that may cause unsolvable interference. Take, for example, in contrast to the traditional scheduling strategy, A is allowed

to transmit  $b$  in time slot 3. Then, B will receive a mixed signal of  $a$  and  $b$ . Since B has received  $a$  before time slot 3, B can recover the data of  $b$  from the mixed signal through our algorithms developed later. In the next time slot, B can forward the recovered  $b$  to the next relay C. Node C will then receive the mixed signal of  $a$  and  $b$  in time slot 4 and recover  $b$  using the same method as before. In time slot 5, node A will transmit another frame of data, namely,  $c$ , and so on. It can be seen that if the data stream is incessant, it will take an average of two time slots to transmit one frame. Compared to with the one third frames per time slot in traditional scheduling, the throughput is significantly increased.

### 2.1 Network Block Codes

Consider for a moment a simple unicast scenario shown in Fig.4 assume that the source is connected to the destination through  $h$  edge-disjoint paths each consisting of unit-capacity edges, and that any  $t$  of these edges can introduce errors. Note that an error can propagate only through the path on which it is introduced. Therefore, the receiver will observe at most  $t$  corrupted symbols, and the source can send information at rate  $k$  to the receiver by the means of an  $(h, k, 2t + 1)$  channel block code that maps  $k$  information symbols to  $h$  coded symbols, and can correct any  $t$  random errors. The coded symbols will be sent simultaneously on the  $h$  edges, thus using the “space” as the resource to accommodate for the redundancy introduced by the code, rather than time as in classical channel coding where coded symbols are sent sequentially and errors occur at different time slots. Consider now a multicast scenario where a source is connected to multiple receivers through an arbitrary network with the min-cut between the source and each receiver equal to  $h$ . Note that if different sets of  $h$  edge disjoint paths between the source and different receivers do not overlap, network coding is not necessary, and the problem reduces to that of Fig. 4 for each receiver separately, and thus to classical channel coding. Otherwise, we want to design the network code to protect the source message for each receiver.

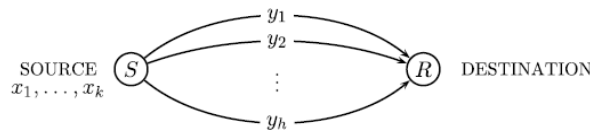


Fig. 4. Simple unicast scenario

**Definition.** A network code is  $t$ -error correcting if it enables each receiver to correctly receive source information as long as the number of edges that introduce errors is smaller than  $t$ . Unlike classical channel codes, network error correction codes use coding operations not only at the source, but also at intermediate nodes of the network. Therefore, an error introduced at a single edge may propagate throughout the network. For simplicity we will assume that both the source and the channel (network) alphabet are  $F_q$ . Therefore, Fig. 4 at the source node,  $k$  information symbols are encoded into  $h$  coded symbols, which are then simultaneously transmitted to the destination. The source produces  $q^k$  messages. If the network code is such that each receiver can correctly decode if errors are introduced in up to  $t$  edges, then, for each receiver, the set of  $q^k$   $h$ -dimensional vectors at any  $h$ -cut corresponding to the  $q^k$  different source messages will be an  $(h, k)$  classical code that can correct at least  $t$  errors. Therefore, the appropriate channel coding bounds connecting parameters  $q, h, k,$  and  $t$  hold.

### 2.2 Bit Error Rate (BER):

Bit error Rate, sometimes bit error ratio (BER) is the most fundamental measure of system performance. That is, it is a measure of how well bits are transferred end-to-end. While this performance is affected by factors such as signal-to-noise and distortion, ultimately it is the ability to receive information error-free that defines the quality of the link. Bit error ratio (BER) is the number of bits received in error, divided by the total number of bits received. It is the percentage of bits that have errors relative to the total number of bits received in a transmission, usually expressed as ten to a negative power. For example, a transmission might have a BER of  $10^{-5}$ , meaning that on average, 1 out of every of 100,000 bits transmitted exhibits an error. The BER is an indication of how often a packet or other data unit has to be retransmitted because of an error. If the BER is higher than typically expected for the system, it may indicate that a slower data rate would actually

improve overall transmission time for a given amount of transmitted data since the BER might be reduced, lowering the number of packets that had to be resent. The formulae to calculate the BER are used here as follows:

**Case-I:** In this case, AWGN is generated by using ‘randn’ function and multiplied by noise power data sequence is generated by using ‘randsrc’ function. Received data is obtained by adding AWGN and data bit generated earlier. ‘sign’ function is used to demodulate and recover data in noisy condition. ‘abs’ function is used to find absolute value and complex magnitude.

**Case-II:** In this case, AWGN is generated by using ‘randn’ function and multiplied by signal power data sequence is generated by using ‘randsrc’ function and multiplied by signal power. Received data is obtained by adding AWGN and data bit generated earlier. ‘sign’ function is used to demodulate and recover data in noisy condition and then multiplied by signal power. ‘abs’ function is used to find absolute value and complex magnitude.

To calculate the Bit Error Rate (BER):

$$\begin{aligned} \text{Err\_symbol} &= \text{abs}(\text{recover\_data} - \text{TX\_data}) \\ \text{Total\_err} &= \text{length}(\text{find}(\text{Err\_sysnbol})) \\ \text{BER} &= \text{Total\_err}/N \end{aligned}$$

### III. SIGNAL-RECOVERY ALGORITHM FOR AWGN AND BLOCK-FADING CHANNELS

Additive white Gaussian noise (AWGN) is a channel model in which the only impairment to communication is a linear addition of wideband or white noise with a constant spectral density (expressed as watts per hertz of bandwidth) and a Gaussian distribution of amplitude. The model does not account for fading, frequency selectivity, interference, nonlinearity or dispersion. However, it produces simple and tractable mathematical models which are useful for gaining insight into the underlying behavior of a system before these other phenomena are considered.

#### 3.1 Channel capacity

The AWGN channel is represented by a series of outputs  $Y_i$  at discrete time event index  $i$ .  $Y_i$  is the sum of the input  $X_i$  and noise,  $Z_i$ , where  $Z_i$  is independent and identically distributed and drawn from a zero-mean normal distribution with variance  $n$  (the noise). The  $Z_i$  are further assumed to not be correlated with the  $X_i$ .

$$\begin{aligned} Z_i &\sim N(0, n) \\ Y_i &= X_i + Z_i \sim N(X_i, n) \end{aligned}$$

The capacity of the channel is infinite unless the noise  $n$  is nonzero, and the  $X_i$  is sufficiently constrained. The most common constraint on the input is the so-called "power" constraint, requiring that for a codeword  $(x_1, x_2, \dots, x_k)$  transmitted through the channel, we have:

$$\frac{1}{n} \sum_{i=1}^k x_i^2 \leq P$$

where  $P$  represents the maximum channel power. Therefore, the channel capacity for the power-constrained channel is given by:

$$C = \max_{f(x) \text{ s.t. } E(X^2) \leq P} I(X; Y)$$

Where  $f(x)$  is the distribution of  $X$ . Expand  $I(X; Y)$ , writing it in terms of the differential entropy:

$$I(X; Y) = h(Y) - h(Y/X) = h(Y) - h(X+Z/X) = h(Y) - h(Z/X)$$

But  $X$  and  $Z$  are independent, therefore:

$$I(X; Y) = h(Y) - h(Z)$$

Evaluating the differential entropy of a Gaussian gives:

$$h(Z) = \frac{1}{2} \log(2\pi en)$$

Because X and Z are independent and their sum gives Y:

$$E(Y^2) = E(X + Z)^2 = E(X^2) + 2E(X)E(Z) + E(Z^2) = P + n$$

From this bound, we infer from a property of the differential entropy that

$$h(Y) \leq \frac{1}{2} \log(2\pi e(P + n))$$

Therefore the channel capacity is given by the highest achievable bound on the mutual information:

$$I(X;Y) \leq \frac{1}{2} \log(2\pi e(P + n)) - \frac{1}{2} \log(2\pi en)$$

Where  $I(X;Y)$  is maximized when:

$$X \sim N(0, P)$$

Thus the channel capacity C for the AWGN channel is given by:

$$C = \frac{1}{2} \log\left(1 + \frac{P}{n}\right)$$

### 3.2 Channel capacity and sphere packing

Suppose that we are sending messages through the channel with index ranging from 1 to M, the number of distinct possible messages. If we encode the M messages to  $n$  bits, then we define the rate R as:

$$R = \frac{\log M}{n}$$

A rate is said to be achievable if there is a sequence of codes so that the maximum probability of error tends to zero as  $n$  approaches infinity. The capacity C is the highest achievable rate. Consider a codeword of length  $n$  sent through the AWGN channel with noise level N. When received, the codeword vector variance is now N, and its mean is the codeword sent. The vector is very likely to be contained in a sphere of radius  $\sqrt{n(N + \varepsilon)}$  around the codeword sent. If we decode by mapping every message received onto the codeword at the center of this sphere, then an error occurs only when the received vector is outside of this sphere, which is very unlikely.

Each codeword vector has an associated sphere of received codeword vectors which are decoded to it and each such sphere must map uniquely onto a codeword. Because these spheres therefore must not intersect, we are faced with the problem of sphere packing. How many distinct code words can we pack into our  $n$ -bit codeword vector? The received vectors have a maximum energy of  $n(P+N)$  and therefore must occupy a sphere of radius  $\sqrt{n(P+N)}$ . Each codeword sphere has radius  $\sqrt{nN}$ . The volume of an  $n$ -dimensional sphere is directly proportional to  $r^n$ , so the maximum number of uniquely decodable spheres that can be packed into our sphere with transmission power P is:

$$\frac{(n(P+N))^{\frac{n}{2}}}{(nN)^{\frac{n}{2}}} = 2^{\frac{n}{2} \log(1+P/N)}$$

By this argument, the rate R can be no more than  $\frac{1}{2} \log(1 + P/N)$ .

In the following section, we shall develop the signal-recovery algorithm in AWGN and block-fading channels. In the following discussion, we assume that each frame has  $L$  symbols and that the delay  $D$  of relative to  $\vec{y}$  is an integer and uniformly distributed on  $[-L, L]$ . In the following two parts, we will present the algorithms on recovering  $\vec{y}$  from the mixed signal  $\vec{x} \otimes \vec{y}$  for BPSK and  $\pi/4$  for QPSK modulations, respectively. For other types of linear modulation, the principle of the recovery algorithm is similar.

### 3.3. Signal Recovery for BPSK Modulation

For BPSK modulation, the signals of  $\bar{x}$  and  $\bar{y}$  can mathematically be written as  $Ax(t - D) \cos(\omega t + \gamma)$  and  $By(t) \cos(\omega t)$ , respectively, where  $x(t), y(t) \in \{1, -1\}$ , and  $\gamma$  is the phase shift of the carrier of  $\bar{x}$  from that of  $\bar{y}$ .  $A$  and  $B$  are the signal amplitudes of  $\bar{x}$  and  $\bar{y}$ , respectively. Thus, the mixed signal of  $\bar{x}$  and  $\bar{y}$  at node  $R_2$  can be represented by

$$r(t) = By(t) \cos(\omega t) + Ax(t - D) \cos(\omega t + \gamma).$$

After demodulation and filtering, the sampled signal value of each symbol is

$$s_k = By_k + Ax_{k-D} \cos \gamma + n_k \quad (4)$$

where  $k$  is the sampling index, and  $n_k$  is the additive Gaussian noise with variance  $\sigma^2 n = N_0/2$ . For simplicity, let  $y_k = x_k = 0$  for  $k \in [-L + 1, 0) \cup [L, 2L)$ . We also assume that the carrier phase of  $\bar{y}$  and the local oscillator are ideally synchronized, and the impact of carrier-phase errors will be discussed later in Section V. Since the terminal  $R_2$  has received  $\bar{x}$  before, it can regenerate the sampling signal  $xk$  for  $0 \leq k < L$ . Then, one can compute the correlation between  $\{s_k\}$  and the delayed signal  $\{x_{k-d}\}$ , where  $d \in (-L, L)$  is an integer, to estimate  $A$  and  $D$ . That is

$$\begin{aligned} R(\bar{s}, \bar{x}, d) &= \sum_{k=-L}^{2L-1} s_k x_{k-d} \\ &= B \sum_{k=-L}^{2L-1} y_k x_{k-d} + \sum_{k=-L}^{2L-1} n_k x_{k-d} \\ &\quad + A' \sum_{k=-L}^{2L-1} x_{k-D} x_{k-d} \end{aligned} \quad (5)$$

where  $A' = A \cos \gamma$ . Through effective source coding and channel coding,  $x_k$  and  $y_k$  will take the value of  $\{-1, 1\}$  with equal probability and are independent of each other. Thus, we are satisfied that

$$\begin{aligned} E \left( \sum_{k=-L}^{2L-1} y_k x_{k-d} \right) &= 0 \\ E \left( \sum_{k=-L}^{2L-1} n_k x_{k-d} \right) &= 0 \\ E \left( \sum_{k=-L}^{2L-1} x_{k-D} x_{k-d} \right) &= \begin{cases} L, & d = D \\ 0, & d \neq D. \end{cases} \end{aligned} \quad (6)$$

According to the law of large numbers, if the frame length  $L$  is sufficiently large,  $\sum_{k=-L}^{2L-1} y_k x_{k-d} / L$  and  $\sum_{k=-L}^{2L-1} n_k x_{k-d} / L$  will converge to 0 with very high probabilities. Moreover

$$A' \sum_{k=-L}^{2L-1} x_{k-D} x_{k-d} / L \xrightarrow{L \rightarrow \infty} \begin{cases} A', & d = D \\ 0, & d \neq D \end{cases} \quad (7)$$

is valid with a probability close to 1. Therefore, if one computes  $|R(\bar{s}, \bar{x}, d)|$  for each  $d \in (-L, L)$  and find out the maximum value, a reasonable estimation of  $A$  and  $D$  can be obtained by

$$\hat{A} = R(\bar{s}, \bar{x}, \hat{D}) / L \quad (8)$$

where  $\hat{D} = \arg \max_{-L < d < L} |R(\bar{s}, \bar{x}, d)|$ . By subtracting the estimated signal of  $\bar{x}$  from  $\bar{s}$ ,  $\bar{y}$  can be recovered by

$$\hat{y}_k = s_k - \hat{A} x_{k-\hat{D}} \quad (\max\{0, D\} \leq k < \min\{L, L + D\}). \quad (9)$$

Note that if there are  $h$  frames of interference signals denoted by  $\bar{x}^1, \bar{x}^2, \dots, \bar{x}^h$  instead of only one  $\bar{x}$ , all the interferences can be eliminated by repeating the aforementioned process for  $h$  times. Here is a simplified description of this algorithm.

**Algorithm 1:** Signal-Recovery Algorithm for BPSK in AWGN and Block-Fading Channels.

**Step 0:** Set  $d_j = -L + 1, \hat{A}_j = 0$  for  $j = 1 \sim h$ .  
 Set  $\hat{y}_k = s_k$  for  $k = 0 \sim L - 1$ .

**Step 1:** For  $j = 1 \sim h$   
 For  $d_j = -L + 1 \sim L - 1$   
 Compute  $R(\bar{s}, \bar{x}^j, d_j)$  according to (5).  
 If  $|\hat{A}_j| < |R(\bar{s}, \bar{x}^j, d_j)|$   
 $\hat{A}_j = R(\bar{s}, \bar{x}^j, d_j)/L;$   
 $\hat{D}_j = d_j.$

**Step 2:** For  $j = 1 \sim h$   
 For  $k = \max\{0, \hat{D}_j\} \sim \min\{L, L + \hat{D}_j\}$   
 $\hat{y}_k = \hat{y}_k - \hat{A}_j x_{k-\hat{D}_j}.$

### 3.4 Recovering Algorithm for $\pi/4$ -QPSK Modulation

$\pi/4$ -QPSK modulation is widely used in wireless communications. For  $\pi/4$ -QPSK modulation, the input bit stream is partitioned by a serial-to-parallel converter into two parallel data streams  $m_{I,k}$  and  $m_{Q,k}$ , each with a symbol rate equal to half that of the incoming bit rate. Thus, we assume that the frame length is  $2L$  symbols for convenience. Then, the signal of  $\pi/4$ -QPSK is given by

$$\begin{aligned} s_{\pi/4\text{-QPSK}}(t) &= I(t) \cos(\omega t) - Q(t) \sin(\omega t) \\ &= \cos(\omega t + \theta_k) \end{aligned} \quad (10)$$

where  $\theta_k = \theta_{k-1} + \phi_k$ , and  $\phi_k \in \{\pi/4, -\pi/4, 3\pi/4, -3\pi/4\}$  is related to  $m_{I,k}$  and  $m_{Q,k}$  according to a certain mapping rule. Hence, the mixed signal at node B is

$$s(t) = B \cos(\omega t + \theta_{y_k}) + A \cos(\omega t + \theta_{x_{k-D}} + \gamma) + n(t)$$

where  $\gamma$  is the phase difference between the carriers of  $\bar{x}$  and  $\bar{y}$ .  $D$  is the delay of  $\bar{x}$  relative to  $\bar{y}$ , whereas  $B$  and  $A$  are the attenuations. Suppose that the phase shift of the local carrier from the carrier of  $\bar{y}$  is  $\alpha$ . Then, after demodulation, the sampled in-phase and quadrature signals are

$$I_{s_k} = B \cos(\theta_{y_k} - \alpha) + A \cos(\theta_{x_{k-D}} + \gamma - \alpha) + n_{I,k} \quad (11a)$$

$$Q_{s_k} = B \sin(\theta_{y_k} - \alpha) + A \sin(\theta_{x_{k-D}} + \gamma - \alpha) + n_{Q,k} \quad (11b)$$

respectively.  $n_{I,k}$  and  $n_{Q,k}$  are the Gaussian noises with mean 0. Similarly to BPSK, the sampled signal values of  $\bar{x}$  and  $\bar{y}$  are set to be 0 if  $k < 0$  or  $k \geq L$ . The principle of signal recovery is similar to that for BPSK, and we make use of the correlation between  $s(t)$  and  $\bar{x}$ . First, node  $R_2$  maps  $\bar{x}$  to  $\{\theta_{x_k}\}_{k=0}^{L-1}$  according to the same rule at the transmitter. Then, let

$$\begin{aligned}
 R_I(\vec{s}, \vec{x}, d) &= \sum_{k=-L}^{2L-1} (I_{s_k} \cos \theta_{x_{k-d}} + Q_{s_k} \sin \theta_{x_{k-d}}) \\
 &= B \sum_{k=-L}^{2L-1} \cos(\theta_{y_k} - \theta_{x_{k-d}} - \alpha) \\
 &\quad + \sum_{k=-L}^{2L-1} n_{I,k} \cos \theta_{x_{k-d}} + \sum_{k=-L}^{2L-1} n_{Q,k} \sin \theta_{x_{k-d}} \\
 &\quad + A \sum_{k=-L}^{2L-1} \cos(\theta_{x_{k-D}} - \theta_{x_{k-d}} + \gamma - \alpha) \quad (12a)
 \end{aligned}$$

$$\begin{aligned}
 R_Q(\vec{s}, \vec{x}, d) &= \sum_{k=-L}^{2L-1} (I_{s_k} \sin \theta_{x_{k-d}} - Q_{s_k} \cos \theta_{x_{k-d}}) \\
 &= -B \sum_{k=-L}^{2L-1} \sin(\theta_{y_k} - \theta_{x_{k-d}} - \alpha) \\
 &\quad + \sum_{k=-L}^{2L-1} n_{I,k} \sin \theta_{x_{k-d}} - \sum_{k=-L}^{2L-1} n_{Q,k} \cos \theta_{x_{k-d}} \\
 &\quad - A \sum_{k=-L}^{2L-1} \sin(\theta_{x_{k-D}} - \theta_{x_{k-d}} + \gamma - \alpha). \quad (12b)
 \end{aligned}$$

In (12a),  $\left( B \sum_{k=-L}^{2L-1} \cos(\theta_{y_k} - \theta_{x_{k-d}} - \alpha) + \sum_{k=-L}^{2L-1} n_{I,k} \cos \theta_{x_{k-d}} + \sum_{k=-L}^{2L-1} n_{Q,k} \sin \theta_{x_{k-d}} \right) / L$  converges to 0 as  $L \rightarrow \infty$  with a probability of 1. Moreover

$$\begin{aligned}
 &A \sum_{k=-L}^{2L-1} \cos(\theta_{x_{k-D}} - \theta_{x_{k-d}} + \gamma - \alpha) / L \\
 &\quad \rightarrow \begin{cases} A \cos(\gamma - \alpha), & d = D \\ 0, & d \neq D \end{cases} \quad (L \rightarrow \infty) \quad (13)
 \end{aligned}$$

is valid with a probability of 1. Then, the estimated value of  $A \cos(\gamma - \alpha)$  is given by

$$\hat{A}_I = R_I(\vec{s}, \vec{x}, \hat{D}) / L. \quad (14)$$

Similarly, one can estimate  $A \sin(\gamma - \alpha)$  from (12b) by

$$\hat{A}_Q = -R_Q(\vec{s}, \vec{x}, \hat{D}) / L. \quad (15)$$

In the preceding equations

$$\hat{D} = \arg \max_{-L < d < L} \sqrt{R_I^2(\vec{s}, \vec{x}, d) + R_Q^2(\vec{s}, \vec{x}, d)} / L.$$

Hence, the interference of  $\vec{x}$  can be eliminated from the mixed signal  $s(t)$  as follows:

$$\hat{I}_{y_k} = I_{s_k} - \hat{A}_I \cos(\theta_{x_{k-\hat{D}}}) + \hat{A}_Q \sin(\theta_{x_{k-\hat{D}}}) \quad (16a)$$

$$\hat{Q}_{y_k} = Q_{s_k} - \hat{A}_I \sin(\theta_{x_{k-\hat{D}}}) - \hat{A}_Q \cos(\theta_{x_{k-\hat{D}}}). \quad (16b)$$

Finally, one can decode  $\hat{I}_{yk}$ ,  $\hat{Q}_{yk}$  and recover the original data of  $\bar{y}$  through base band differential detection. Since this technique only computes  $\theta_{yk} - \theta_{y_{k-1}}$  for each  $k$  and the constant phase error  $\alpha$  has no effect on the decoding result, phase synchronization is not required here. In the aforementioned two algorithms, the searching range of  $d$  is set to be  $(-L, L)$ . In fact, it is not necessary to check all the values between  $-L$  and  $L$ . The start and end times of a frame can be found out through its head and tailing bits, respectively. Then, the length of the frame can be figured out. Although accurate duration of the mixed signal is difficult to detect, one can still get an approximate estimation. In addition, whether  $D > 0$  or  $D < 0$  can be decided by checking the identifier in the frame head. Thus, the searching range of  $d$  can greatly be shortened. For example, if we have detected  $D > 0$  and the duration of the mixed signal is quite probably between  $N - l/2$  and  $N + l/2$  symbols. Thus, the start time of  $\bar{x}$  is just  $L$  symbols before the termination time of the mixed signal, so  $D$  is probably between  $N - l/2 - L$  and  $N + l/2 - L$ . Therefore, one can only consider  $d \in [N - l/2 - L, N + l/2 - L]$ , where  $l$  is a predefined parameter. The larger  $l$  is, the larger the probability of  $D \in [N - l/2 - L, N + l/2 - L]$  is. This way, the estimation of  $D$  will be more accurate, and the complexity can largely be reduced.

#### IV. SIGNAL-RECOVERY ALGORITHM FOR TIME-VARIANT CHANNELS

In time-variant channels, the attenuation is not constant during one frame; thus, we need to estimate the signal amplitude of each symbol of  $\bar{x}$ . However, if the channel slowly varies, the signal amplitude can still be estimated by calculating the correlation. An easy and reasonable way is to calculate the glide correlation between  $\bar{x}$  and  $\bar{s}$ . Suppose that the coherent time of the channel is the duration of  $M$  symbols. The signal amplitude  $A_i$  of  $x_i$  can be worked out by calculating the local correlation value as

$$R_i(\bar{s}, \bar{x}, \hat{D}) = \sum_{k=\hat{D}+i-\frac{M}{2}}^{\hat{D}+i+\frac{M}{2}-1} s_k x_{k-\hat{D}} \quad (17)$$

For  $M/2 \leq i < L - M/2$ . Then, let  $\hat{A}_i = R_i / M$  be the estimated signal amplitude of  $x_i$ . Here is the algorithm for BPSK. (For  $\pi/4$ -QPSK and other types of modulations, the ideas are the same).

**Algorithm 2:** Glide Correlation Algorithm on Signal Recovery for BPSK in Time Variant Channels.

**Step 0:** Initialization by setting  $\hat{A} = 0$ .  
**If**  $D > 0$   
 Let  $D_1 = N - L - l/2$ ,  $D_2 = N - L + l/2$ ;  
**Else**  
 Let  $D_1 = L - N - l/2$ ,  $D_2 = L - N + l/2$ ;

**Step 1:** Find out the delay of  $\bar{x}$  relative to  $\bar{y}$  as follows.  
**For**  $d = D_1 \sim D_2$   
 Compute  $R = \sum_{i=d}^{d+L-1} |\sum_{k=i}^{i+M-1} s_k x_{k-d}| / M$   
**If**  $\hat{A} < R$   
 $\hat{A} = R$ ;  
 $\hat{D} = d$ .

**Step 2:** Calculate the amplitude of  $\bar{x}$  as follows.  
**For**  $i = 0 \sim L - 1$   
**If**  $i < \lceil M/2 \rceil$   
 $A_i = \sum_{k=\hat{D}}^{\hat{D}+M-1} s_k x_{k-\hat{D}} / M$ ;  
**Else if**  $i \geq \lceil L - M/2 \rceil$   
 $A_i = \sum_{k=L+\hat{D}-M}^{L+\hat{D}-1} s_k x_{k-\hat{D}} / M$ ;  
**Else**  
 $A_i = \sum_{k=\hat{D}+i-M/2}^{\hat{D}+i+M/2-1} s_k x_{k-\hat{D}} / M$ .

**Step 3:** **For**  $k = \hat{D} \sim \hat{D} + L - 1$ , eliminate  $\bar{x}$  from  $\bar{s}$  as:  
 $\hat{y}_k = s_k - A_{k-\hat{D}} x_{k-\hat{D}}$ .

If the coherent time  $M$  is relatively small,  $A_i$  may not be accurately estimated through the correlation, and considerable interference may be induced. To deal with this problem, we will propose another signal-

recovery algorithm based on maximum likelihood. Without loss of generality, we shall take BPSK as an example. The received mixed signal of  $\bar{x}$  and  $\bar{y}$  can be represented by

$$s_k = B'_k \cos(\theta_{y_k} + \phi_{y_k}) + A'_{k-D} \cos(\theta_{x_{k-D}} + \phi_{x_{k-D}}) + n_k \quad (18)$$

where  $B'_k$  and  $\phi_{y_k}$  are the amplitude and phase gains of the channel from  $S_2$  to  $R_2$  at the sampling time  $k$ , respectively. Similarly,  $A'_k$  and  $\phi_{x_k}$  are the channel gains from  $S_1$  to  $R_2$ .  $\theta_{y_k}$  and  $\theta_{x_k}$  are the binary phase shifts related to the information bits in  $\bar{x}$  and  $\bar{y}$ , respectively. Since  $\theta_{y_k}$  and  $\theta_{x_k}$  only have two possible values, namely, 0 and  $\pi$ , we have

$$s_k = B'_k \cos \phi_{y_k} \cos \theta_{y_k} + A'_{k-D} \cos \phi_{x_{k-D}} \cos \theta_{x_{k-D}} + n_k. \quad (19)$$

In (19), the attenuations  $B'_k \cos \phi_{y_k}$  and  $A'_k \cos \phi_{x_k}$  are Gaussian random variables modeled by the AR processes. For simplicity, let  $B_k = B'_k \cos \phi_{y_k}$  and  $A_k = A'_k \cos \phi_{x_k}$ . Since  $A_k$ ,  $B_k$ , and  $n_k$  are independent of each other, the joint distribution of the three variables is

$$p(B_k, A_{k-D}, n_k) = \frac{1}{(2\pi)^{3/2} \sigma_{\varepsilon_x} \sigma_{\varepsilon_y} \sigma_n} \times \exp \left\{ -\frac{(B_k - \bar{B}_k)^2}{2\sigma_{\varepsilon_y}^2} - \frac{(A_{k-D} - \bar{A}_{k-D})^2}{2\sigma_{\varepsilon_x}^2} - \frac{n_k^2}{2\sigma_n^2} \right\} \quad (20)$$

where  $\bar{B}_k$  and  $\bar{A}_k$  are the expectations defined as (2), whereas  $\sigma_{\varepsilon_x}$  and  $\sigma_{\varepsilon_y}$  correspond to the variance  $\sigma_{\varepsilon}$  in (2). Note that maximizing the joint probability equates to minimizing the power part in (20). Hence, one only needs to solve the following optimization problem **M**:

$$\begin{aligned} \text{Min } H_{\theta_{y_k}} &= \frac{(B_k - \bar{B}_k)^2}{\sigma_{\varepsilon_y}^2} + \frac{(A_{k-D} - \bar{A}_{k-D})^2}{\sigma_{\varepsilon_x}^2} + \frac{n_k^2}{\sigma_n^2} \\ \text{s.t. } s_k &= B_k \cos \theta_{y_k} + A_{k-D} \cos \theta_{x_{k-D}} + n_k. \end{aligned} \quad (21)$$

Let us normalize the variables in the objective function by setting  $\tilde{A}_{k-D} = (A_{k-D} - \bar{A}_{k-D}) / \sigma_{\varepsilon_x}$ ,  $\tilde{B}_k = (B_k - \bar{B}_k) / \sigma_{\varepsilon_y}$ , and  $\tilde{n}_k = n_k / \sigma_n$ . Then,  $H_{\theta_{y_k}}$  can be regarded as the square of the Euclidean distance from  $\{\tilde{A}_{k-D}, \tilde{B}_k, \tilde{n}_k\}$  to the origin. Let  $s'_k = s_k - \cos \theta_{y_k} \bar{B}_k - \cos \theta_{x_{k-D}} \bar{A}_{k-D}$ ; thus, the solution to the problem **M** is as follows:

$$\begin{cases} \hat{B}_k = \frac{s'_k \sigma_{\varepsilon_y}^2 \cos \theta_{y_k}}{\sigma_{\varepsilon_y}^2 + \sigma_{\varepsilon_x}^2 + \sigma_n^2} + \bar{B}_k \\ \hat{A}_{k-D} = \frac{s'_k \sigma_{\varepsilon_x}^2 \cos \theta_{x_{k-D}}}{\sigma_{\varepsilon_y}^2 + \sigma_{\varepsilon_x}^2 + \sigma_n^2} + \bar{A}_{k-D} \\ \hat{n}_k = \frac{s'_k \sigma_n^2}{\sigma_{\varepsilon_y}^2 + \sigma_{\varepsilon_x}^2 + \sigma_n^2}. \end{cases} \quad (22)$$

After solving (21), one can compute  $\bar{B}_{k+1}$  and  $\bar{A}_{k+1-D}$  as in (2). Then, the amplitude of the signals of  $\bar{x}$  and  $\bar{y}$ , as well as the Gaussian noise, can recursively be figured out. Note that in (22),  $\theta_{y_k}$  is an unknown variable. Fortunately,  $\theta_{y_k}$  has only finite values. One can first calculate  $H_{\theta_{y_k}}$  for  $\theta_{y_k} = 0$  and  $\pi$ , respectively, and then select  $\theta_{y_k} = \arg \min H_{\theta_{y_k}}$  as the decoding result of  $y_k$ .

Note that one needs to know the delay  $D$  before performing the recursive calculation. This can be achieved by the correlation method mentioned in Section III. Another problem is how to calculate the initial values of  $\hat{A}_k$  and  $\hat{B}_k$  for  $k \leq p$  [ $p$  is the order of the AR process defined in (3)]. If  $D > 0$ , which means  $\bar{x}$  is sent later than  $\bar{y}$ , then the foreside of  $\bar{y}$  is not disturbed by  $\bar{x}$ . Since only the destroyed part of  $\bar{y}$  needs signal

recovery, one can set the initial values  $\hat{B}_k = s_k / \cos \theta_{y_k}$  for  $k \leq p$ , whereas the initial values of  $\hat{A}_k$  can be set to be 0. For  $D < 0$ , the strategy is similar. In conclusion, the algorithm can be summarized as follows.

**Algorithm 3:** Signal-Recovery Algorithm by Maximizing the Posterior Probability for BPSK in Time-Variant Channels.

**Step 0:** Calculate  $\hat{D}$  by the correlation operation as Step 1 in Algorithm 2.

**Step 1:** If  $\hat{D} \geq 0$   
 Set  $\hat{B}_k = s_k / \cos \theta_{y_k}$  and  $\hat{A}_{k-\hat{D}} = 0$  for  $\hat{D} - \min\{p, \hat{D}\} \leq k < \hat{D}$ ;  
 Set  $\hat{B}_k = \hat{B}_{\hat{D}-\min\{p, \hat{D}\}}$  and  $\hat{A}_{k-\hat{D}} = 0$  for  $\hat{D} - p \leq k < \hat{D} - \min\{p, \hat{D}\}$ ;  
 Else  
 Set  $\hat{A}_{k-\hat{D}} = s_{k-\hat{D}} / \cos \theta_{x_{k-\hat{D}}}$  and  $\hat{B}_k = 0$  for  $\max\{-p, -\hat{D}\} \leq k < 0$ ;  
 Set  $\hat{A}_{k-\hat{D}} = \hat{A}_{\max\{-p, -\hat{D}\}}$  and  $\hat{B}_k = 0$  for  $-p \leq k < \max\{-p, -\hat{D}\}$ .

**Step 2:** For  $k = \max\{0, \hat{D}\} \sim \min\{L - \hat{D}, L\}$   
 Set  $\theta_{y_k} = 0$  and calculate  $H_{0,k}$  according to (21) and (22);  
 Set  $\theta_{y_k} = \pi$  and calculate  $H_{\pi,k}$  according to (21) and (22).  
 If  $H_{0,k} < H_{\pi,k}$   
 $\theta_{y_k} = 0$ ;  
 Else  
 $\theta_{y_k} = \pi$ .  
 Calculate  $\hat{B}_k, \hat{A}_{k-\hat{D}}, \hat{n}_k$  according to (22).

**Step 3:** For  $k = \hat{D} \sim \hat{D} + L - 1$   
 Subtract the signal of  $\bar{x}$  from the mixed signal as  
 $\hat{y}_k = s_k - \hat{A}_{k-\hat{D}} x_{k-\hat{D}}$ .

Considering the errors in the aforementioned estimation of the initial values of  $A_k$  and  $B_k$ , we will adopt the following method to improve the recovery result: First, Algorithm 3 is performed. Then, the obtained  $\{\hat{B}_k\}$  and  $\{\hat{A}_{k-D}\}$  are regarded as the initial values of the attenuations. Take  $D > p$ , for example, and let the initial values  $A'_k = s_k / \cos \theta_{x_k}$  and  $B_k = \hat{B}_{L-1}$  for  $L \leq k < L+p$ . Then, we calculate the attenuation values in reverse order from the sampling time  $\min\{L, L+D\}$  to  $\max\{0, D\}$  according to Algorithm 3. After that, we combine the two results and choose the one maximizing the likelihood. This method can make full use of the information in the signal and, thus, can enhance the performance of the algorithm with a relatively high complexity. Since the channel model in (1) is a forward generating equation, the inverted generating function needs to be derived for the reverse computation. Note that the function in (1) is essentially a conditional distribution of a Markovian process, and the joint distribution of multiple Gaussian random variables is still a Gaussian distribution characterized by the covariance matrix and the means of the variables. The inverted generating function can be obtained by calculating the co-variances between the attenuations at different sampling times. For the AR process, however, the problem can be simplified by the following proposition.

*Proposition 4.1:* Given an AR process with mean 0 as in (3), the inverted generating function is

$$A_{n-p} + u_1 A_{n-p+1} + \cdots + u_{p-1} A_{n-1} + u_p A_n = \zeta_{n-p} \quad (23)$$

where  $\zeta_n$  is a purely random Gaussian process with mean 0 and variance  $\sigma_\varepsilon^2$ .

## V. PERFORMANCE ANALYSIS

### 5.1 Performance Analysis

In the following section, we will analyze the performance of the recovery algorithms in the previous sections. Due to the complexity of time-variant channels, we will only derive the analytical results for AWGN and block-fading channels. The performance in time-variant channels will be shown by simulation results in the next section. We shall consider the BER performance and the effect of phase errors, as well as the inter symbol interference (ISI).

#### 5.2.1 BER Performances

First, we consider BPSK modulation. From the correlation algorithm of signal recovery in Section III-A, it can be seen that the resulting error bits in the recovered frame  $\bar{y}$  are mainly due to two factors, namely, the Gaussian noise and estimation errors of  $A$  and  $D$ . If  $\hat{D} = D$ , then from (9)

$$\begin{aligned}\hat{y}_k &= By_k + (A - \hat{A})x_{k-D} + n_k \\ &= By_k + x_{k-D} \sum_{j=D}^{D+L-1} (By_j x_{j-D} + n_j x_{j-D}) / L + n_k.\end{aligned}\quad (24)$$

Thus, the total noise  $n'_k = x_{k-D} \sum_{j=D}^{D+L-1} (By_j x_{j-D} + n_j x_{j-D}) / L + n_k$ . Note that  $x_{k-D} \sum_{j=D}^{D+L-1} n_j x_{j-D} / L$  is a Gaussian random variable with mean 0 and variance  $\sigma_n^2 / L$ . According to the central limit theorem,  $x_{k-D} \sum_{j=D}^{D+L-1} y_j x_{j-D} / L$  can be approximated by a Gaussian variable with mean 0 and variance  $(L - |D|) / L^2 < 1 / L$ . Thus, the variance of  $n'_k$  is smaller than  $\sigma_{n'}^2 = \sigma_n^2 + \sigma_n^2 / L + B^2 / L$ . Thus the conditional BER satisfies.

$$P_e(\hat{D} = D) \leq Q\left(\frac{B}{\sigma_{n'}}\right) = Q\left(\sqrt{\frac{LB^2}{L\sigma_n^2 + \sigma_n^2 + B^2}}\right).\quad (25)$$

If  $L$  is large enough and the signal-to-noise ratio (SNR) of the channel is relatively small, the noise induced by the correlation operation has a little effect on the total SNR and the BER performance. Consider the probability  $P(\hat{D} \neq D)$  subsequently. Suppose  $d \in [D - l/2, D + l/2]$ , then

$$\begin{aligned}P(\hat{D} \neq D) &= 1 - P(R(\bar{\mathbf{s}}, \bar{\mathbf{x}}, D)) \\ &> R(\bar{\mathbf{s}}, \bar{\mathbf{x}}, d), d \in \left[D - \frac{l}{2}, D\right] \cap \left[D, \frac{D+l}{2}\right] \\ &\leq \sum_{\substack{d=D-1/2 \\ d \neq D}}^{D+1/2} P(R(\bar{\mathbf{s}}, \bar{\mathbf{x}}, D) < R(\bar{\mathbf{s}}, \bar{\mathbf{x}}, d)) \\ &\leq lQ\left(\frac{|A|}{\sigma_z}\right)\end{aligned}\quad (26)$$

Where  $\sigma_z^2 = (A^2 + 2B^2 + 2\sigma_n^2) / L$ . According to (25) and (26), given  $A$ ,  $B$ , and  $\sigma_n^2$ , the upper bound of the BER is

$$\begin{aligned}P_e(A, B, \sigma_n) &= P(\hat{D} = D)P(\text{error}|\hat{D} = D) \\ &\quad + P(\hat{D} \neq D)P(\text{error}|\hat{D} \neq D) \\ &\leq P(\text{error}|\hat{D} = D) + P(\hat{D} \neq D) \\ &\leq Q\left(\frac{B}{\sigma_{n'}}\right) + lQ\left(\frac{|A|}{\sigma_z}\right) \\ &= Q\left(\sqrt{\frac{LB^2}{L\sigma_n^2 + \sigma_n^2 + B^2}}\right) \\ &\quad + lQ\left(\sqrt{\frac{LA^2}{A^2 + 2B^2 + 2\sigma_n^2}}\right).\end{aligned}\quad (27)$$

From (27), it can be seen that the larger  $L$  is, the better the BER performance is. If  $L$  is large enough, the noise induced by calculating the correlation can be neglected. For the block-fading channel, where  $A$  and  $B$  are random variables, the upper bound of the BER is given by

$$P_e = \int_A \int_B P_e(A, B, \sigma_n) p_A(A) p_B(B) dA dB \quad (28)$$

where  $p_A(A)$  and  $p_B(B)$  are the Rayleigh distribution functions of  $A$  and  $B$ , respectively. The BER analysis of  $\pi/4$ -QPSK in AWGN and block-fading channels is similar to that of BPSK. It must also be noted that there may be error bits in  $\bar{x}$  itself, and this will impact  $P(\hat{D} = D)$  and increase the BER of  $\bar{y}$ . Hence, it is necessary to adopt a reliable channel coding scheme to avoid the propagation of error bits.

### 5.2.2 Impact of the Synchronization Error

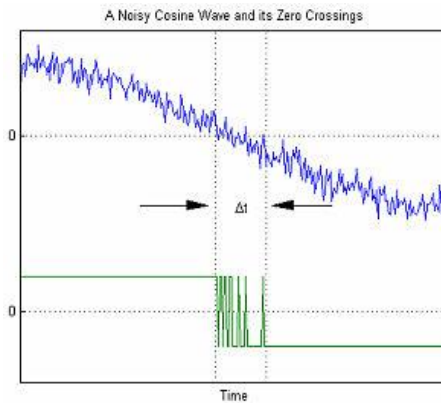
Since the baseband differential detection technique only detects the phase difference between the previous and current samples, the constant phase shift  $\alpha$  will not affect the demodulation result of  $\pi/4$ -QPSK. However, for BPSK, the phase error of the local carrier will reduce the power of the received signal and result in BER performance degradation. Assume that in (4), the phase difference between  $\bar{y}$  and the local carrier is  $\gamma_y$ , and that between  $\bar{x}$  and the local carrier is  $\gamma_x$ . After coherent demodulation, the sampled signal is

$$s_k = B y_k \cos \gamma_y + A x_{k-D} \cos \gamma_x + n_k.$$

After eliminating  $\bar{x}$  from the mixed signal  $\bar{s}$ , the power loss of  $\bar{y}$  is  $\cos^2 \gamma_y$ . Suppose that  $\gamma_y$  is uniformly distributed on  $[-\pi, \pi]$ , then the average power loss is

$$\frac{1}{2\pi} \int_{-\pi}^{\pi} \cos^2 \gamma_y d\gamma_y = 0.5 = -3 \text{ dB}. \quad (29)$$

However, if differential PSK is adopted, the BER degradation due to the phase error is less than 1 dB for large SNRs.



### 5.2 Effects in time domain (time variant)

In serial data communications, the AWGN mathematical model is used to model the timing error caused by random jitter (RJ). The graph to the right shows an example of timing errors associated with AWGN. The variable  $\Delta t$  represents the uncertainty in the zero crossing. As the amplitude of the AWGN is increased, the signal-to-noise ratio decreases. This results in increased uncertainty  $\Delta t$ . When affected by AWGN, The average number of either positive going or negative going zero-crossings per second at the output of a narrow band pass filter when the input is a sine wave is:

$$\frac{\text{positive zero crossings}}{\text{second}} = \frac{\text{negative zero crossings}}{\text{second}}$$

$$= f_0 \sqrt{\frac{\text{SNR} + 1 + \frac{B^2}{12f_0^2}}{\text{SNR} + 1}}$$

Where

- $f_0$  = the center frequency of the filter
- $B$  = the filter bandwidth
- $\text{SNR}$  = the signal-to-noise power ratio in linear terms

Fig. 9. Zero-Crossings of a Noisy Cosine

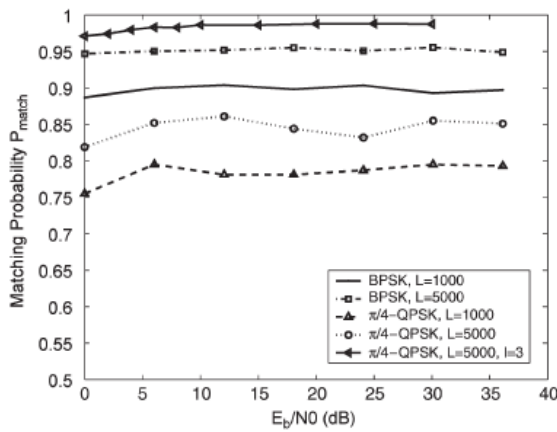
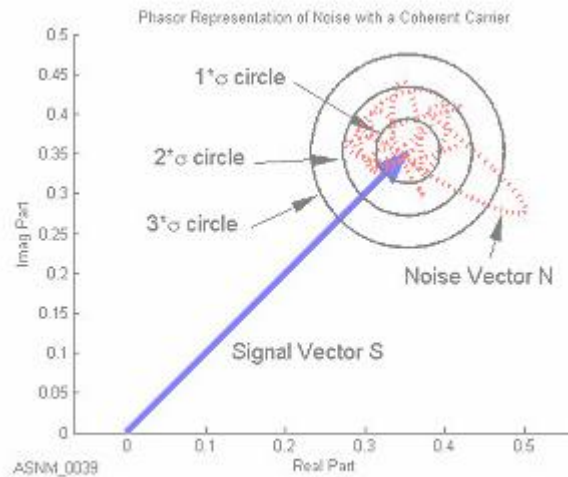
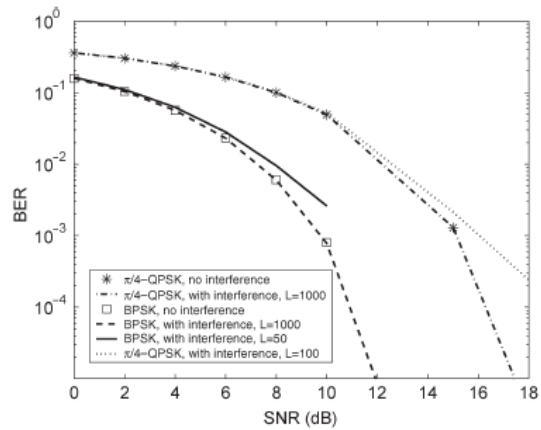
## 5.2 Effects in phasor domain

In modern communication systems, band limited AWGN cannot be ignored. When modeling band limited AWGN in the phasor domain, statistical analysis reveals that the amplitudes of the real and imaginary contributions are independent variables which follow the Gaussian distribution model. When combined, the resultant phasor's magnitude is a Rayleigh distributed random variable while the phase is uniformly distributed from 0 to  $2\pi$ .

The graph to the right shows an example of how band limited AWGN can affect a coherent carrier signal. The instantaneous response of the Noise Vector cannot be precisely predicted; however its time-averaged response can be statistically predicted. As shown in the graph, we confidently predict that the noise phasor will reside inside the  $1\sigma$  circle about 38% of the time; the noise phasor will reside inside the  $2\sigma$  circle about 86% of the time; and the noise phasor will reside inside the  $3\sigma$  circle about 98% of the time.

## VI. SIMULATION RESULTS

In this section, we will present the sample simulation results to further investigate the performance of the proposed signal recovery algorithms. In the simulation, we adopt the network model shown in Fig. 3, where  $\bar{y}$  is the desired information, and  $\bar{x}$  acts as the interference. The delay of  $\bar{x}$  relative to  $\bar{y}$  is uniformly distributed in  $[-L, L]$ . In block-fading channels, the amplitudes of  $\bar{y}$  and  $\bar{x}$  are set to be independent Rayleigh random variables with variance 1. In AWGN channels, the amplitude of  $\bar{y}$  is set to be constant 1 and that of  $\bar{x}$  is set to be a random variable uniformly distributed in  $[-1, 1]$ . Fig. 4 shows the matching probability  $P(\hat{D} = D)$  versus different frame lengths for both BPSK and  $\pi/4$ -QPSK modulations in the AWGN channel. In this figure, we set  $d \in [-L, L]$ . It can be seen that  $P(\hat{D} = D)$  increases as  $L$  becomes larger, which is consistent with the theoretical analysis. For the frame length  $L = 5000$ ,  $P(\hat{D} = D)$  is more than 95% for BPSK and 90% for  $\pi/4$ -QPSK. This matching probability is acceptable since most wireless frames are not very short. The mismatching cases mainly result from the fact that the amplitude of  $\bar{x}$  is too small. In these cases,  $\bar{x}$  brings about little interference to  $\bar{y}$  and, thus, can be treated as common noise. Note the matching probability for BPSK is larger than that for  $\pi/4$ -QPSK, and this is mainly because for BPSK,  $y_k x_{k-d}$  has only two possible values, namely, 1 and  $-1$ . Whereas for  $\pi/4$ -QPSK,  $\cos(\theta_{y_k} - \theta_{x_{k-d}} - \alpha)$  and  $\sin(\theta_{y_k} - \theta_{x_{k-d}} - \alpha)$  have eight possible values, respectively. Thus, the variance of  $R(\bar{s}, \bar{x}, d)$  ( $d \neq D$ ) in (5) is much smaller than that in (12). Fig. 5 shows the probability  $P(\hat{D} = D)$  under different SNRs. It can be seen that the power of noise has little impact on


 Fig. 5. Probability of  $\hat{D} = D$  versus different SNRs in an AWGN channel.

 Fig. 6. BER performance for BPSK and  $\pi/4$ -QPSK versus different SNRs in an AWGN channel.

$P(\hat{D} = D)$  under large frame lengths and moderate SNRs. The uppermost curve is the result of the method mentioned in the last paragraph in Section III with  $l = 3$ , and the match probability is much larger than that with  $d \in [-L, L]$ . Figs. 6 and 7 illustrate the BER performance of the recovery algorithms under different SNRs for AWGN and block-fading channels, respectively. For BPSK modulation,  $\text{SNR} = B^2 / \sigma_n^2$ , where  $B$  is the amplitude of  $\vec{y}$ , and  $\sigma_n^2$  is the power of the additive white noise. For  $\pi/4$ -QPSK, we define  $\text{SNR} = B^2 / \sigma_n^2$ , where  $\sigma_n^2$  is the variance of both  $n_{I,k}$  and  $n_{Q,k}$  in (11). Note that this definition is different from the standard definition of SNR for  $\pi/4$ -QPSK; thus, there is a constant shift from the curves of  $\pi/4$ -QPSK to that of BPSK. In Fig. 6, the BER of the algorithm with small  $L$  is larger than that with big  $L$  under high SNRs. Moreover, the transmission without interference and that with interference but adopting our recovery algorithm have almost the same BER under low SNRs, even if  $L$  is as small as 100. Fig. 7 shows the similar result in Rayleigh block-fading channels. Thus, the two figures indicate that the algorithm will bring about little additional noise to the desired signal if  $L$  is not too small. Therefore, with a proper frame length, the transmission capacity can be approached by our strategy.

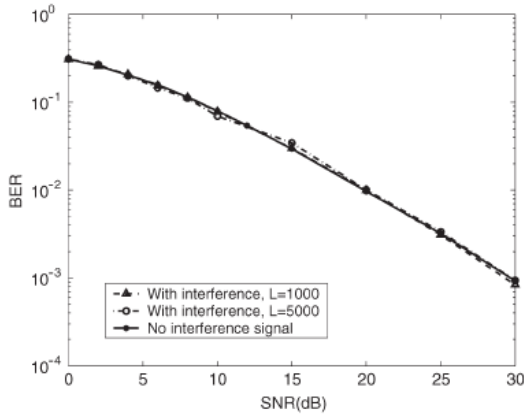


Fig. 7. BER performance for  $\pi/4$ -QPSK versus different SNRs in a block-fading channel.

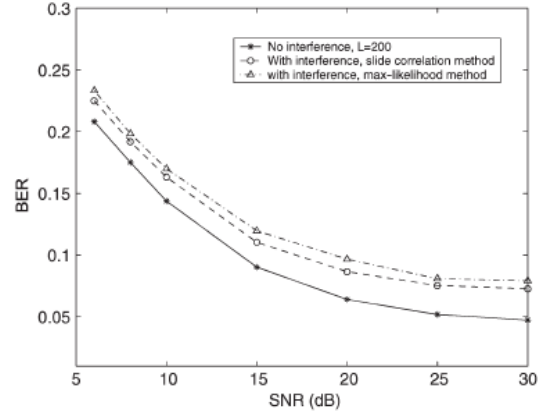


Fig. 8. BER performance for BPSK versus different SNRs in a time-variant channel.

Fig. 8 shows the BER performance of the two algorithms in Section IV in a time-variant channel. The star curve is for the scenario with no interference. The BER curves with circles and triangles are obtained through Algorithms 2 and 3, respectively. Here, we use an AR process  $A_n - 0.99A_{n-1} = \varepsilon_n$  as the channel model. We set  $\sqrt{\text{Var}(A_n)} = 10$ , and thus,  $\sigma_\varepsilon = 1.41$ . Again, the delay  $D \in [-L, L]$ . Comparing the value of  $\sigma_\varepsilon$  with  $\sqrt{\text{Var}(A_n)}$ , one can see that the attenuation of the channel varies rather rapidly. From our simulation, the attenuation value changes from positive to negative within an average duration of about 20 symbols. From the simulation result it is shown that our algorithms are able to remove almost all the interference.

## VII. CONCLUSION

In this paper, we have proposed a signal-recovery scheme based on the physical-layer network coding, which can eliminate the interference signal and recover the useful information from the mixed signal. By this scheme, a new scheduling strategy, which allows a certain kind of signal collision without division techniques, can be realized, and the throughput in wireless networks can greatly be increased. We have developed the signal-recovery algorithms for AWGN, block-fading, and time-variant channels, respectively. For AWGN and block fading channels, we made use of the correlation between the known information and the received signals at the relay nodes to separate the desired signal from the mixed signal. For time variant channels, if the coherent time is large enough, a glide correlation operation can eliminate the interference signal. A key feature of the proposed physical layer network coding strategy is that neither synchronization nor power control among the different transmitters is needed, thus making it well suited for distributed networks. By making of Theoretical analysis and simulation results have shown that the signal-recovery algorithms can largely eliminate the interference from the mixed signal.

## REFERENCES

- [1] A. Bachir, D. Barthel, M. Heusse, and A. Duda, "Hidden nodes avoidance in wireless sensor networks," in Proc. Int. Conf. Wireless Netw., Commun. Mobile Comput., Jun. 13–16, 2005, pp. 612–617
- [2] Kaveh Pahlavan, "Wireless information networks examines sensor and mobile ad-hoc networks", International journal of wireless information, ISSN: 1068-9605, 2010, J.No. 10776
- [3] T. C. Keong, presented at the Ad hoc mobile wireless networks: Protocols Syst. Conf., 2002.
- [4] S. A. Aly and A. E. Kamal. Network protection codes against link failures using network coding. In Proc. Of IEEE 2008 Global Telecommunications Conference, Dec. 2008.
- [5] Morgan Kaufmann, "Wireless Communications and Networking", Jul 28, 2010
- [6] Jochen H. Schiller. "Mobile Communications", Addison-Wesley, 2003
- [7] Theodore S. Rappaport, "Wireless Communications – Principles and Practice", Dorling Kindersley, 2009
- [8] IETF "Mobile ad-hoc Networks (manet), <http://www.ietf.org/html.charters/manet-charter.html>
- [9] Wireless Networking and Mobile IP", [http://www.cse.wustl.edu/~jain/refs/wir\\_book.html](http://www.cse.wustl.edu/~jain/refs/wir_book.html)
- [10] Wireless Networking – online references", "Mobile multimedia and communication", <http://www.mobile3q.com/>, <http://www.wirelessadvisor.com>.
- [11] Rober Spalding, "Storage Networks: The Complete Reference", ISBN: 0072224762, McGraw-Hill/Osborne © 2003.